

# Elliptic flow for $\phi$ mesons and (anti)deuterons in Au+Au collisions at $\sqrt{s_{NN}} = 200$ GeV

S. Afanasiev,<sup>17</sup> C. Aidala,<sup>7</sup> N.N. Ajitanand,<sup>43</sup> Y. Akiba,<sup>37,38</sup> J. Alexander,<sup>43</sup> A. Al-Jamel,<sup>33</sup> K. Aoki,<sup>23,37</sup> L. Aphecetche,<sup>45</sup> R. Armendariz,<sup>33</sup> S.H. Aronson,<sup>3</sup> R. Averbeck,<sup>44</sup> T.C. Awes,<sup>34</sup> B. Azmoun,<sup>3</sup> V. Babintsev,<sup>14</sup> A. Baldisseri,<sup>8</sup> K.N. Barish,<sup>4</sup> P.D. Barnes,<sup>26</sup> B. Bassalleck,<sup>32</sup> S. Bathe,<sup>4</sup> S. Batsouli,<sup>7</sup> V. Baublis,<sup>36</sup> F. Bauer,<sup>4</sup> A. Bazilevsky,<sup>3</sup> S. Belikov,<sup>3,16</sup> R. Bennett,<sup>44</sup> Y. Berdnikov,<sup>40</sup> M.T. Bjonrdal,<sup>7</sup> J.G. Boissevain,<sup>26</sup> H. Borel,<sup>8</sup> K. Boyle,<sup>44</sup> M.L. Brooks,<sup>26</sup> D.S. Brown,<sup>33</sup> D. Bucher,<sup>29</sup> H. Buesching,<sup>3</sup> V. Bumazhnov,<sup>14</sup> G. Bunce,<sup>3,38</sup> J.M. Burward-Hoy,<sup>26</sup> S. Butsyk,<sup>44</sup> S. Campbell,<sup>44</sup> J.-S. Chai,<sup>18</sup> S. Chernichenko,<sup>14</sup> J. Chiba,<sup>19</sup> C.Y. Chi,<sup>7</sup> M. Chiu,<sup>7</sup> I.J. Choi,<sup>52</sup> T. Chujo,<sup>49</sup> V. Cianciolo,<sup>34</sup> C.R. Clevelin,<sup>12</sup> Y. Cobigo,<sup>8</sup> B.A. Cole,<sup>7</sup> M.P. Comets,<sup>35</sup> P. Constantin,<sup>16</sup> M. Csanád,<sup>10</sup> T. Csörgő,<sup>20</sup> T. Dahms,<sup>44</sup> K. Das,<sup>11</sup> G. David,<sup>3</sup> H. Delagrange,<sup>45</sup> A. Denisov,<sup>14</sup> D. d'Enterria,<sup>7</sup> A. Deshpande,<sup>38,44</sup> E.J. Desmond,<sup>3</sup> O. Dietzsch,<sup>41</sup> A. Dion,<sup>44</sup> J.L. Drachenberg,<sup>1</sup> O. Drapier,<sup>24</sup> A. Drees,<sup>44</sup> A.K. Dubey,<sup>51</sup> A. Durum,<sup>14</sup> V. Dzhordzhadze,<sup>46</sup> Y.V. Efremenko,<sup>34</sup> J. Egdemir,<sup>44</sup> A. Enokizono,<sup>13</sup> H. En'yo,<sup>37,38</sup> B. Espagnon,<sup>35</sup> S. Esumi,<sup>48</sup> D.E. Fields,<sup>32,38</sup> F. Fleuret,<sup>24</sup> S.L. Fokin,<sup>22</sup> B. Forestier,<sup>27</sup> Z. Fraenkel,<sup>51</sup> J.E. Frantz,<sup>7</sup> A. Franz,<sup>3</sup> A.D. Frawley,<sup>11</sup> Y. Fukao,<sup>23,37</sup> S.-Y. Fung,<sup>4</sup> S. Gadrat,<sup>27</sup> F. Gastineau,<sup>45</sup> M. Germain,<sup>45</sup> A. Glenn,<sup>46</sup> M. Gonin,<sup>24</sup> J. Gosset,<sup>8</sup> Y. Goto,<sup>37,38</sup> R. Granier de Cassagnac,<sup>24</sup> N. Grau,<sup>16</sup> S.V. Greene,<sup>49</sup> M. Grosse Perdekamp,<sup>15,38</sup> T. Gunji,<sup>5</sup> H.-Å. Gustafsson,<sup>28</sup> T. Hachiya,<sup>13,37</sup> A. Hadj Henni,<sup>45</sup> J.S. Haggerty,<sup>3</sup> M.N. Hagiwara,<sup>1</sup> H. Hamagaki,<sup>5</sup> H. Harada,<sup>13</sup> E.P. Hartouni,<sup>25</sup> K. Haruna,<sup>13</sup> M. Harvey,<sup>3</sup> E. Haslum,<sup>28</sup> K. Hasuko,<sup>37</sup> R. Hayano,<sup>5</sup> M. Heffner,<sup>25</sup> T.K. Hemmick,<sup>44</sup> J.M. Heuser,<sup>37</sup> X. He,<sup>12</sup> H. Hiejima,<sup>15</sup> J.C. Hill,<sup>16</sup> R. Hobbs,<sup>32</sup> M. Holmes,<sup>49</sup> W. Holzmann,<sup>43</sup> K. Homma,<sup>13</sup> B. Hong,<sup>21</sup> T. Horaguchi,<sup>37,47</sup> M.G. Hur,<sup>18</sup> T. Ichihara,<sup>37,38</sup> K. Imai,<sup>23,37</sup> M. Inaba,<sup>48</sup> D. Isenhower,<sup>1</sup> L. Isenhower,<sup>1</sup> M. Ishihara,<sup>37</sup> T. Isobe,<sup>5</sup> M. Issah,<sup>43</sup> A. Isupov,<sup>17</sup> B.V. Jacak,<sup>44,\*</sup> J. Jia,<sup>7</sup> J. Jin,<sup>7</sup> O. Jinnouchi,<sup>38</sup> B.M. Johnson,<sup>3</sup> K.S. Joo,<sup>30</sup> D. Jouan,<sup>35</sup> F. Kajihara,<sup>5,37</sup> S. Kametani,<sup>5,50</sup> N. Kamihara,<sup>37,47</sup> M. Kaneta,<sup>38</sup> J.H. Kang,<sup>52</sup> T. Kawagishi,<sup>48</sup> A.V. Kazantsev,<sup>22</sup> S. Kelly,<sup>6</sup> A. Khanzadeev,<sup>36</sup> D.J. Kim,<sup>52</sup> E. Kim,<sup>42</sup> Y.-S. Kim,<sup>18</sup> E. Kinney,<sup>6</sup> A. Kiss,<sup>10</sup> E. Kistenev,<sup>3</sup> A. Kiyomichi,<sup>37</sup> C. Klein-Boesing,<sup>29</sup> L. Kochenda,<sup>36</sup> V. Kochetkov,<sup>14</sup> B. Komkov,<sup>36</sup> M. Konno,<sup>48</sup> D. Kotchetkov,<sup>4</sup> A. Kozlov,<sup>51</sup> P.J. Kroon,<sup>3</sup> G.J. Kunde,<sup>26</sup> N. Kurihara,<sup>5</sup> K. Kurita,<sup>39,37</sup> M.J. Kweon,<sup>21</sup> Y. Kwon,<sup>52</sup> G.S. Kyle,<sup>33</sup> R. Lacey,<sup>43</sup> J.G. Lajoie,<sup>16</sup> A. Lebedev,<sup>16</sup> Y. Le Bornec,<sup>35</sup> S. Leckey,<sup>44</sup> D.M. Lee,<sup>26</sup> M.K. Lee,<sup>52</sup> M.J. Leitch,<sup>26</sup> M.A.L. Leite,<sup>41</sup> H. Lim,<sup>42</sup> A. Litvinenko,<sup>17</sup> M.X. Liu,<sup>26</sup> X.H. Li,<sup>4</sup> C.F. Maguire,<sup>49</sup> Y.I. Makdisi,<sup>3</sup> A. Malakhov,<sup>17</sup> M.D. Malik,<sup>32</sup> V.I. Manko,<sup>22</sup> H. Masui,<sup>48</sup> F. Matathias,<sup>44</sup> M.C. McCain,<sup>15</sup> P.L. McGaughey,<sup>26</sup> Y. Miake,<sup>48</sup> T.E. Miller,<sup>49</sup> A. Milov,<sup>44</sup> S. Mioduszewski,<sup>3</sup> G.C. Mishra,<sup>12</sup> J.T. Mitchell,<sup>3</sup> D.P. Morrison,<sup>3</sup> J.M. Moss,<sup>26</sup> T.V. Moukhanova,<sup>22</sup> D. Mukhopadhyay,<sup>49</sup> J. Murata,<sup>39,37</sup> S. Nagamiya,<sup>19</sup> Y. Nagata,<sup>48</sup> J.L. Nagle,<sup>6</sup> M. Naglis,<sup>51</sup> T. Nakamura,<sup>13</sup> J. Newby,<sup>25</sup> M. Nguyen,<sup>44</sup> B.E. Norman,<sup>26</sup> A.S. Nyanin,<sup>22</sup> J. Nystrand,<sup>28</sup> E. O'Brien,<sup>3</sup> C.A. Ogilvie,<sup>16</sup> H. Ohnishi,<sup>37</sup> I.D. Ojha,<sup>49</sup> H. Okada,<sup>23,37</sup> K. Okada,<sup>38</sup> O.O. Omiwade,<sup>1</sup> A. Oskarsson,<sup>28</sup> I. Otterlund,<sup>28</sup> K. Ozawa,<sup>5</sup> D. Pal,<sup>49</sup> A.P.T. Palounek,<sup>26</sup> V. Pantuev,<sup>44</sup> V. Papavassiliou,<sup>33</sup> J. Park,<sup>42</sup> W.J. Park,<sup>21</sup> S.F. Pate,<sup>33</sup> H. Pei,<sup>16</sup> J.-C. Peng,<sup>15</sup> H. Pereira,<sup>8</sup> V. Peresedov,<sup>17</sup> D.Yu. Peressounko,<sup>22</sup> C. Pinkenburg,<sup>3</sup> R.P. Pisani,<sup>3</sup> M.L. Putschke,<sup>3</sup> A.K. Purwar,<sup>44</sup> H. Qu,<sup>12</sup> J. Rak,<sup>16</sup> I. Ravinovich,<sup>51</sup> K.F. Read,<sup>34,46</sup> M. Reuter,<sup>44</sup> K. Reygers,<sup>29</sup> V. Riabov,<sup>36</sup> Y. Riabov,<sup>36</sup> G. Roche,<sup>27</sup> A. Romana,<sup>24,†</sup> M. Rosati,<sup>16</sup> S.S.E. Rosendahl,<sup>28</sup> P. Rosnet,<sup>27</sup> P. Rukoyatkin,<sup>17</sup> V.L. Rykov,<sup>37</sup> S.S. Ryu,<sup>52</sup> B. Sahlmueller,<sup>29</sup> N. Saito,<sup>23,37,38</sup> T. Sakaguchi,<sup>5,50</sup> S. Sakai,<sup>48</sup> V. Samsonov,<sup>36</sup> H.D. Sato,<sup>23,37</sup> S. Sato,<sup>3,19,48</sup> S. Sawada,<sup>19</sup> V. Semenov,<sup>14</sup> R. Seto,<sup>4</sup> D. Sharma,<sup>51</sup> T.K. Shea,<sup>3</sup> I. Shein,<sup>14</sup> T.-A. Shibata,<sup>37,47</sup> K. Shigaki,<sup>13</sup> M. Shimomura,<sup>48</sup> T. Shohjoh,<sup>48</sup> K. Shoji,<sup>23,37</sup> A. Sickles,<sup>44</sup> C.L. Silva,<sup>41</sup> D. Silvermyr,<sup>34</sup> K.S. Sim,<sup>21</sup> C.P. Singh,<sup>2</sup> V. Singh,<sup>2</sup> S. Skutnik,<sup>16</sup> W.C. Smith,<sup>1</sup> A. Soldatov,<sup>14</sup> R.A. Soltz,<sup>25</sup> W.E. Sondheim,<sup>26</sup> S.P. Sorensen,<sup>46</sup> I.V. Sourikova,<sup>3</sup> F. Staley,<sup>8</sup> P.W. Stankus,<sup>34</sup> E. Stenlund,<sup>28</sup> M. Stepanov,<sup>33</sup> A. Ster,<sup>20</sup> S.P. Stoll,<sup>3</sup> T. Sugitate,<sup>13</sup> C. Suire,<sup>35</sup> J.P. Sullivan,<sup>26</sup> J. Sziklai,<sup>20</sup> T. Tabaru,<sup>38</sup> S. Takagi,<sup>48</sup> E.M. Takagui,<sup>41</sup> A. Taketani,<sup>37,38</sup> K.H. Tanaka,<sup>19</sup> Y. Tanaka,<sup>31</sup> K. Tanida,<sup>37,38</sup> M.J. Tannenbaum,<sup>3</sup> A. Taranenko,<sup>43</sup> P. Tarján,<sup>9</sup> T.L. Thomas,<sup>32</sup> M. Togawa,<sup>23,37</sup> J. Tojo,<sup>37</sup> H. Torii,<sup>37</sup> R.S. Towell,<sup>1</sup> V.-N. Tram,<sup>24</sup> I. Tserruya,<sup>51</sup> Y. Tsuchimoto,<sup>13,37</sup> S.K. Tuli,<sup>2</sup> H. Tydesjö,<sup>28</sup> N. Tyurin,<sup>14</sup> H. Valle,<sup>49</sup> H.W. vanHecke,<sup>26</sup> J. Velkovska,<sup>49</sup> R. Vertesi,<sup>9</sup> A.A. Vinogradov,<sup>22</sup> E. Vznuzdaev,<sup>36</sup> M. Wagner,<sup>23,37</sup> X.R. Wang,<sup>33</sup> Y. Watanabe,<sup>37,38</sup> J. Wessels,<sup>29</sup> S.N. White,<sup>3</sup> N. Willis,<sup>35</sup> D. Winter,<sup>7</sup> C.L. Woody,<sup>3</sup> M. Wysocki,<sup>6</sup> W. Xie,<sup>4,38</sup> A. Yanovich,<sup>14</sup> S. Yokkaichi,<sup>37,38</sup> G.R. Young,<sup>34</sup> I. Younus,<sup>32</sup> I.E. Yushmanov,<sup>22</sup> W.A. Zajc,<sup>7</sup> O. Zaudtke,<sup>29</sup> C. Zhang,<sup>7</sup> J. Zimányi,<sup>20,†</sup> and L. Zolin<sup>17</sup>

(PHENIX Collaboration)

<sup>1</sup>Abilene Christian University, Abilene, TX 79699, U.S.

- <sup>2</sup>Department of Physics, Banaras Hindu University, Varanasi 221005, India  
<sup>3</sup>Brookhaven National Laboratory, Upton, NY 11973-5000, U.S.  
<sup>4</sup>University of California - Riverside, Riverside, CA 92521, U.S.  
<sup>5</sup>Center for Nuclear Study, Graduate School of Science, University of Tokyo, 7-3-1 Hongo, Bunkyo, Tokyo 113-0033, Japan  
<sup>6</sup>University of Colorado, Boulder, CO 80309, U.S.  
<sup>7</sup>Columbia University, New York, NY 10027 and Nevis Laboratories, Irvington, NY 10533, U.S.  
<sup>8</sup>Dapnia, CEA Saclay, F-91191, Gif-sur-Yvette, France  
<sup>9</sup>Debrecen University, H-4010 Debrecen, Egyetem tér 1, Hungary  
<sup>10</sup>ELTE, Eötvös Loránd University, H - 1117 Budapest, Pázmány P. s. 1/A, Hungary  
<sup>11</sup>Florida State University, Tallahassee, FL 32306, U.S.  
<sup>12</sup>Georgia State University, Atlanta, GA 30303, U.S.  
<sup>13</sup>Hiroshima University, Kagamiyama, Higashi-Hiroshima 739-8526, Japan  
<sup>14</sup>IHEP Protvino, State Research Center of Russian Federation, Institute for High Energy Physics, Protvino, 142281, Russia  
<sup>15</sup>University of Illinois at Urbana-Champaign, Urbana, IL 61801, U.S.  
<sup>16</sup>Iowa State University, Ames, IA 50011, U.S.  
<sup>17</sup>Joint Institute for Nuclear Research, 141980 Dubna, Moscow Region, Russia  
<sup>18</sup>KAERI, Cyclotron Application Laboratory, Seoul, South Korea  
<sup>19</sup>KEK, High Energy Accelerator Research Organization, Tsukuba, Ibaraki 305-0801, Japan  
<sup>20</sup>KFKI Research Institute for Particle and Nuclear Physics of the Hungarian Academy of Sciences (MTA KFKI RMKI), H-1525 Budapest 114, POBox 49, Budapest, Hungary  
<sup>21</sup>Korea University, Seoul, 136-701, Korea  
<sup>22</sup>Russian Research Center “Kurchatov Institute”, Moscow, Russia  
<sup>23</sup>Kyoto University, Kyoto 606-8502, Japan  
<sup>24</sup>Laboratoire Leprince-Ringuet, Ecole Polytechnique, CNRS-IN2P3, Route de Saclay, F-91128, Palaiseau, France  
<sup>25</sup>Lawrence Livermore National Laboratory, Livermore, CA 94550, U.S.  
<sup>26</sup>Los Alamos National Laboratory, Los Alamos, NM 87545, U.S.  
<sup>27</sup>LPC, Université Blaise Pascal, CNRS-IN2P3, Clermont-Fd, 63177 Aubiere Cedex, France  
<sup>28</sup>Department of Physics, Lund University, Box 118, SE-221 00 Lund, Sweden  
<sup>29</sup>Institut für Kernphysik, University of Muenster, D-48149 Muenster, Germany  
<sup>30</sup>Myongji University, Yongin, Kyonggido 449-728, Korea  
<sup>31</sup>Nagasaki Institute of Applied Science, Nagasaki-shi, Nagasaki 851-0193, Japan  
<sup>32</sup>University of New Mexico, Albuquerque, NM 87131, U.S.  
<sup>33</sup>New Mexico State University, Las Cruces, NM 88003, U.S.  
<sup>34</sup>Oak Ridge National Laboratory, Oak Ridge, TN 37831, U.S.  
<sup>35</sup>IPN-Orsay, Université Paris Sud, CNRS-IN2P3, BP1, F-91406, Orsay, France  
<sup>36</sup>PNPI, Petersburg Nuclear Physics Institute, Gatchina, Leningrad region, 188300, Russia  
<sup>37</sup>RIKEN, The Institute of Physical and Chemical Research, Wako, Saitama 351-0198, Japan  
<sup>38</sup>RIKEN BNL Research Center, Brookhaven National Laboratory, Upton, NY 11973-5000, U.S.  
<sup>39</sup>Physics Department, Rikkyo University, 3-34-1 Nishi-Ikebukuro, Toshima, Tokyo 171-8501, Japan  
<sup>40</sup>Saint Petersburg State Polytechnic University, St. Petersburg, Russia  
<sup>41</sup>Universidade de São Paulo, Instituto de Física, Caixa Postal 66318, São Paulo CEP05315-970, Brazil  
<sup>42</sup>System Electronics Laboratory, Seoul National University, Seoul, South Korea  
<sup>43</sup>Chemistry Department, Stony Brook University, Stony Brook, SUNY, NY 11794-3400, U.S.  
<sup>44</sup>Department of Physics and Astronomy, Stony Brook University, SUNY, Stony Brook, NY 11794, U.S.  
<sup>45</sup>SUBATECH (Ecole des Mines de Nantes, CNRS-IN2P3, Université de Nantes) BP 20722 - 44307, Nantes, France  
<sup>46</sup>University of Tennessee, Knoxville, TN 37996, U.S.  
<sup>47</sup>Department of Physics, Tokyo Institute of Technology, Oh-okayama, Meguro, Tokyo 152-8551, Japan  
<sup>48</sup>Institute of Physics, University of Tsukuba, Tsukuba, Ibaraki 305, Japan  
<sup>49</sup>Vanderbilt University, Nashville, TN 37235, U.S.  
<sup>50</sup>Waseda University, Advanced Research Institute for Science and Engineering, 17 Kikui-cho, Shinjuku-ku, Tokyo 162-0044, Japan  
<sup>51</sup>Weizmann Institute, Rehovot 76100, Israel  
<sup>52</sup>Yonsei University, IPAP, Seoul 120-749, Korea

(Dated: November 6, 2018)

Differential elliptic flow ( $v_2$ ) for  $\phi$  mesons and (anti)deuterons ( $\bar{d}$ ) $d$  is measured for Au+Au collisions at  $\sqrt{s_{NN}} = 200$  GeV. The  $v_2$  for  $\phi$  mesons follows the trend of lighter  $\pi^\pm$  and  $K^\pm$  mesons, suggesting that ordinary hadrons interacting with standard hadronic cross sections are not the primary driver for elliptic flow development. The  $v_2$  values for ( $\bar{d}$ ) $d$  suggest that elliptic flow is additive for composite particles. This further validation of the universal scaling of  $v_2$  per constituent quark for baryons and mesons suggests that partonic collectivity dominates the transverse expansion dynamics.

An important goal of current ultra-relativistic heavy ion research is to map out the accessible regions of the Quantum Chromodynamics (QCD) phase diagram. Central to this goal, is the creation and study of a new phase of nuclear matter – the Quark Gluon Plasma (QGP). Thermalization and de-confinement are important properties of this matter, believed to be produced in heavy ion collisions at the Relativistic Heavy Ion Collider (RHIC) [1, 2, 3].

Detailed elliptic flow measurements provide indispensable information about this high energy density matter [4, 5, 6, 7, 8]. Such measurements are characterized by the magnitude of the second-harmonic coefficient  $v_2 = \langle e^{i2(\varphi_p - \Phi_{RP})} \rangle$ , of the Fourier expansion of the azimuthal distribution of emitted particles. Here,  $\varphi_p$  represents the azimuthal emission angle of a particle,  $\Phi_{RP}$  is the azimuthal angle of the reaction plane and the brackets denote statistical averaging over particles and events [9, 10].

At RHIC energies, there is now significant evidence that elliptic flow, in non-central collisions, results from hydrodynamic pressure gradients developed in a locally thermalized “almond-shaped” collision zone. That is, the initial transverse coordinate-space anisotropy of this zone is converted, via particle interactions, into an azimuthal momentum-space anisotropy. Indeed, when plotted as a function of the transverse kinetic energy  $KE_T \equiv m_T - m$  divided by the number of valence quarks  $n_q$ , of a given hadron ( $n_q = 2$  for mesons and  $n_q = 3$  for baryons),  $v_2/n_q$  shows universal scaling for a broad range of particle species [11, 12, 13] ( $m_T$  is the transverse mass). This has been interpreted as evidence that hydrodynamic expansion of the QGP occurs during a phase characterized by (i) a rather low viscosity to entropy ratio  $\eta/s$  [2, 3, 13, 14, 15] and (ii) independent quasi-particles which exhibit the quantum numbers of quarks [13, 16, 17, 18, 19, 20]. A consensus on the detailed dynamical evolution of the QGP has not been reached [3, 15].

Elliptic flow measurements for heavy, strange and multi-strange hadrons [21, 22] can lend unique insight on reaction dynamics. Here, we use differential  $v_2$  measurements for the  $\phi$  meson and the deuteron to address the important question of how the existence of a hadronic phase affects  $v_2$ , i.e whether or not elliptic flow development is dominantly pre- or post-hadronization.

The  $\phi$  meson is comprised of a strange ( $s$ ) and an anti-strange ( $\bar{s}$ ) quark and its interaction with hadrons is suppressed according to the Okubo-Zweig-Izuka (OZI) rules [23]. One consequence of this is that the  $\phi$  meson is expected to have a rather small hadronic cross section with non-strange hadrons ( $\sim 9$  mb) [24, 25, 26]. Such a cross-section leads to a relatively large mean free path  $\lambda_\phi$ , when compared to the transverse size of the emitting system [13, 20]. Thus, if elliptic flow was established in a phase involving hadrons interacting with their standard

hadronic cross sections (post-hadronization), one would expect  $v_2$  for the  $\phi$  meson to be significantly smaller than that for other hadrons (e.g.  $p$  and  $\pi$ ). If  $v_2$  is established in the phase prior to hadronization, the  $\phi$  meson provides an important benchmark test for universal scaling in that its mass is similar to that of the proton and the  $\Lambda$  baryon, but its  $v_2$  should be additive with respect to the  $v_2$  of its two constituent quarks (i.e.  $n_q = 2$ ). Therefore, a detailed comparison of the  $v_2$  values for the  $\phi$  meson with those for other particle species, comprised of the lighter  $u$  and  $d$  quarks or the heavier charm quark  $c$ , can provide unique insight on whether or not partonic collectivity plays a central role in reaction dynamics at RHIC [19, 27, 28].

The deuteron is a very shallow composite  $p+n$  bound state, whose binding energy ( $\sim 2.24$  MeV) is much less than the hadronization temperature. Thus, it is likely that it would suffer from medium induced breakup in the hadronic phase, even if it was produced at hadronization. In fact, recent investigations [29, 30] suggest that  $(\bar{p}n)pn$  coalescence dominates the (anti)deuteron  $(\bar{d})d$  yield in Au+Au collisions. Thus,  $v_2$  measurements for  $(\bar{d})d$  also provide an important test for the universal scaling of elliptic flow [27] in that its  $v_2$  should be additive; first, with respect to the  $v_2$  of its constituent hadrons and second, with respect to the  $v_2$  of the constituent quarks of these hadrons, i.e.  $n_q = 2 \times 3$ .

In the 2004 running period the PHENIX detector [31] recorded  $\approx 6.5 \times 10^8$  minimum-bias events for Au+Au collisions at  $\sqrt{s_{NN}} = 200$  GeV. The collision vertex  $z$  (along beam axis) was constrained to  $|z| < 30$  cm of the nominal crossing point. The event centrality was determined via cuts in the space of Beam-Beam Counter (BBC) charge versus Zero Degree Calorimeter energy [32]. In the central rapidity region ( $|\eta| \leq 0.35$ ) the drift chambers, each with an azimuthal coverage  $\Delta\varphi = \pi/2$ , and two layers of multi-wire proportional chambers with pad readout (PC1 and PC3) were used for charged particle tracking and momentum reconstruction. The time-of-flight (TOF) and lead scintillator (PbSc) detectors were used for charged particle identification [6, 7].

Time-of-flight measurements from the TOF and PbSc were used in conjunction with the measured momentum and flight-path length, to generate a mass-squared ( $m^2$ ) distribution [33]. A track confirmation hit within a  $2.5\sigma$  matching window in PC3 or TOF/PbSc served to eliminate most albedo, conversions, and resonance decays. A momentum dependent  $\pm 2\sigma$  cut about each peak in the  $m^2$  distribution was used to identify pions ( $\pi^\pm$ ), kaons ( $K^\pm$ ), (anti)protons ( $(\bar{p})p$ ), and  $(\bar{d})d$  in the range  $0.2 < p_T < 2.5$  GeV/ $c$ ,  $0.3 < p_T < 2.5$  GeV/ $c$ ,  $0.5 < p_T < 4.5$  GeV/ $c$ , and  $1.1 < p_T < 4.5$  GeV/ $c$  respectively in the TOF, and to identify  $K^\pm$  in the range  $0.3 < p_T < 1.5$  GeV/ $c$  in the PbSc. This gives  $\sim 59000$   $\bar{d} + d$ . An invariant mass analysis of the  $\phi \rightarrow K^+K^-$  decay channel yielded  $\sim 340000$   $\phi$  mesons with relatively

good signal to background (14 - 42% for the mass window  $|m_{inv}| = 5$  MeV/ $c^2$  about the  $\phi$  meson peak) over the range  $1.0 < p_T < 5.5$  GeV/ $c$  for  $K^+K^-$  pairs.

The reaction plane method [6] was used to correlate the azimuthal angles of charged tracks with the azimuth of the event plane  $\Phi_2$ , determined via hits in the two BBCs covering the pseudo-rapidity range  $3 < |\eta| < 3.9$ . The large rapidity gap  $\Delta\eta > 2.75$  between the central arms and the particles used for reaction plane determination reduces the influence of possible non-flow contributions, especially those from di-jets [34].

Charge averaged values of  $v_2 = \langle \cos(2(\varphi_p - \Phi_2)) \rangle / \langle \cos(2(\Phi_2 - \Phi_{RP})) \rangle$  were evaluated for  $\pi^\pm$ ,  $K^\pm$ ,  $(\bar{p})p$ , and  $(\bar{d})d$ . Here, the denominator represents a resolution factor which corrects for the difference between the estimated  $\Phi_2$  and the true azimuth  $\Phi_{RP}$  of the reaction plane [6, 35]. The estimated resolution factor of the combined reaction plane from both BBC's has an average of 0.33 over centrality, with a maximum of about 0.42 in mid-central collisions [6, 12]. The associated systematic error is estimated to be  $\sim 5\%$  for  $\pi^\pm$ ,  $K^\pm$ , and  $(\bar{p})p$ . A  $p_T$  dependent correction factor ( $\sim 5 - 11\%$ ) was applied to the  $v_2$  values for  $(\bar{d})d$ , to account for background contributions to the (anti)deuteron peak (signal) in the  $m^2$  distributions (see dashed-dot curve in Fig. 1d):

$$v_2^{(\bar{d})d}(p_T) = \left( v_2^{s+bg}(p_T) - (1 - R)v_2^{bg}(p_T) \right) / R, \quad (1)$$

where  $v_2^{s+bg}(p_T)$  is the measured  $v_2$  for  $(\bar{d})d$  + background at a given  $p_T$ ,  $R$  is the ratio signal/(signal+background) at that  $p_T$ , and  $v_2^{bg}(p_T)$  is the elliptic flow of the background evaluated for  $m^2$  values outside of the  $(\bar{d})d$  peaks.

Extraction of the elliptic flow values for the  $\phi$  meson ( $v_2^\phi$ ) followed the invariant mass ( $m_{inv}$ ) method [36]. For each event,  $m_{inv}$ ,  $p_T^{pair}$ , and  $\varphi^{pair}$  for each  $K^+K^-$  pair were evaluated. Then, for each  $p_T^{pair}$  bin,  $v_2^{pair} = \langle \cos(2(\varphi^{pair} - \Phi_2)) \rangle$  was evaluated as a function of  $m_{inv}$  as shown in Fig. 1c. The value  $v_2^\phi(p_T)$  was then obtained from  $v_2^{pair}(m_{inv})$  via an expression similar to Eq. 1:

$$v_2^{pair}(m_{inv}) = v_2^\phi R(m_{inv}) + v_2^{bg}(m_{inv})(1 - R(m_{inv})), \quad (2)$$

where  $R(m_{inv}) = N_\phi(m_{inv}) / [N_\phi(m_{inv}) + N_{bg}(m_{inv})]$  and  $N_\phi(m_{inv})$  and  $N_{bg}(m_{inv})$  are distributions for the  $\phi$  meson and the combinatoric background, respectively.  $N_\phi(m_{inv})$  is obtained from the distribution  $N_{pair}(m_{inv})$  of  $K^+K^-$  pairs from the same event (foreground);  $N_{bg}(m_{inv})$  is the distribution of pairs obtained from different events with similar centrality, vertex, and event plane orientation [37]. Figure 1(a) shows a representative example of the latter distributions for  $1.6 \leq p_T^{pair} \leq 2.7$  GeV/ $c$  and reaction centrality 20-60%. A clear peak signaling the  $\phi$  meson is apparent in the foreground distribution for  $m_{inv} \sim 1.02$  GeV/ $c^2$ . The background distribution was normalized to that for the foreground in

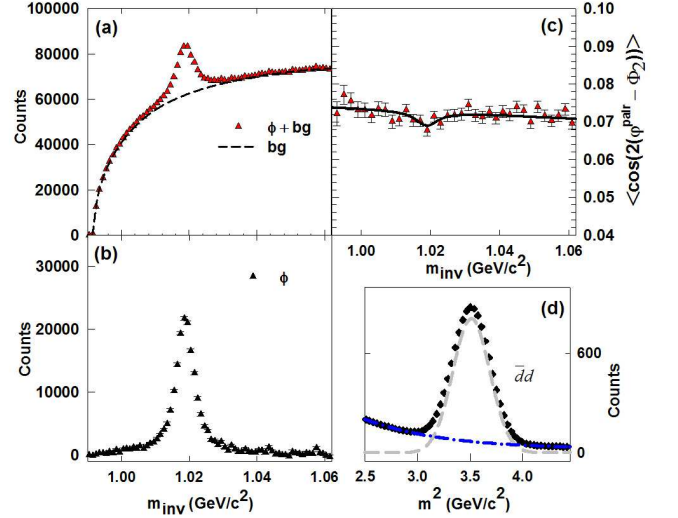


FIG. 1: (a)  $m_{inv}$  distributions for foreground (points) and background (dashed-line)  $K^+K^-$  pairs ( $p_T^{pair} = 1.6 - 2.7$  GeV/ $c$ ) for 20-60% central Au+Au collisions. (b)  $m_{inv}$  distribution after subtraction of the background; (c)  $\langle \cos(2(\varphi^{pair} - \Phi_2)) \rangle$  vs.  $m_{inv}$ ; the solid line is a fit to the data with Eq. 2. (d)  $m^2$  distribution for  $\bar{d}, d$  for  $p_T = 1.6 - 2.9$  GeV/ $c$ .

the region  $1.04 < m_{inv} < 1.2$  GeV/ $c^2$  and subtracted to obtain the  $N_\phi(m_{inv})$  distribution shown in Fig. 1(b); a relatively narrow  $\phi$  meson peak is apparent.

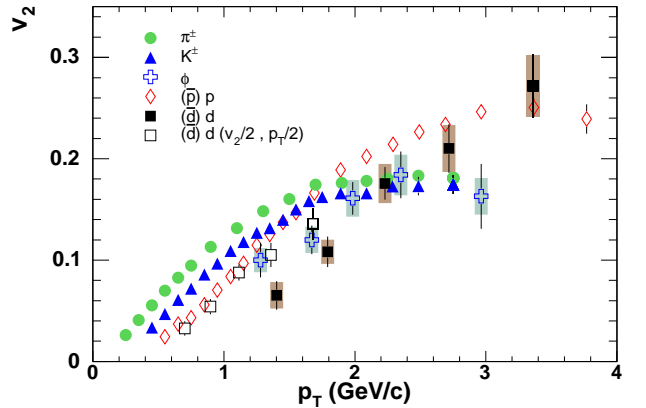


FIG. 2: (color online) Comparison of differential  $v_2(p_T)$  for  $\phi$  mesons,  $(\bar{d})d$ ,  $\pi^\pm$ ,  $K^\pm$ , and  $(\bar{p})p$  (as indicated). Results are shown for 20-60% central Au+Au collisions.

Determination of the ratio  $R(m_{inv})$  was facilitated by fitting this distribution with a Breit-Wigner plus a linear function, as shown by the solid curve in Fig. 1(c). To ensure robust  $v_2^\phi$  extraction, the combinatorial background was constructed such that  $v_2^{bg}(m_{inv})$  gave the same value as  $v_2^{pair}(m_{inv})$  for  $m_{inv}$  values not associated with the  $\phi$  meson peak. Values for  $v_2^\phi$  were extracted via direct

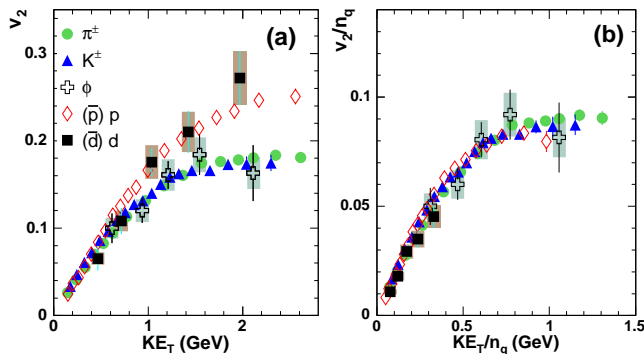


FIG. 3: (color online)(a)  $v_2$  vs  $KE_T$  for several identified particle species obtained in mid-central (20-60%) Au+Au collisions. (b)  $v_2/n_q$  vs  $KE_T/n_q$  for the same particle species shown in panel (a). The shaded bands indicate systematic error estimates for  $(\bar{d})d$  and  $\phi$  mesons (see text).

fits to the  $v_2^{\text{pair}}(m_{inv})$  distribution for each  $p_T^{\text{pair}}$  selection (cf. Eq. 2). That is,  $v_2^{\text{bg}}(m_{inv})$  was parametrized as a linear or quadratic function of  $m_{inv}$  (depending on the  $p_T^{\text{pair}}$  bin) and  $v_2^\phi$  was taken as a fit parameter.

The accuracy of the extraction procedure was verified by checking that the  $m_{inv}$  dependence of the sine coefficients,  $v_{s,2}^{\text{pair}}(m_{inv}) = \langle \sin(2(\varphi^{\text{pair}} - \Phi_2)) \rangle$ , were all zero within statistical errors. An alternative “subtraction method” [38, 39], in which the raw  $\phi$  meson yield distribution  $dN/d(\varphi_\phi - \Phi_2)$  was extracted and fitted with the function  $N(1 + 2v_2^\phi \cos(2(\varphi_\phi - \Phi_2)))$ , also showed good agreement, albeit with larger error bars;  $N$  is an arbitrary normalization constant.

The differential  $v_2(p_T)$  obtained for  $(\bar{d})d$  and the  $\phi$  meson, for centrality 20 - 60%, are compared to those for  $\pi^\pm$ ,  $K^\pm$ , and  $(\bar{p})p$  in Fig. 2. This centrality selection was so chosen to (i) maximize the  $\phi$  meson signal to background ratio over the full range of  $p_T$  bins and (ii) enhance the distinction between baryon and meson  $v_2$  in the intermediate  $p_T$  range. The shaded bands for  $(\bar{d})d$  and the  $\phi$  meson indicate systematic errors ( $\sim 6 - 15\%$ ), primarily associated with the determination of  $R$  and  $R(m_{inv})$ ,  $v_2^{\text{bg}}$  and  $v_2^{\text{bg}}(m_{inv})$  (cf. Eqs. 1 and 2), and fitting.

The values for  $v_2^{(\bar{d})d}$  shown in Fig. 2 are as much as a factor  $\approx 2.5$  lower than those for  $\pi^\pm$  at low  $p_T$ . This mass ordering pattern reflects the detailed expansion dynamics of the created matter. As a first test of whether or not  $v_2$  for  $(\bar{d})d$  is additive with respect to its constituent hadrons,  $v_2^{(\bar{d})d}/2$  vs.  $p_T/2$  is compared to  $v_2^{(\bar{p})p}$  vs.  $p_T$ . Within errors, they show good agreement as would be expected if  $v_2^{(\bar{d})d}$  is additive. Another salient feature of the results shown is the large magnitude of  $v_2$  for the  $\phi$  meson, which gives an initial indication that significant flow development occurs prior to hadronization.

The left and right panels of Fig. 3 compare the un-

scaled and scaled results (respectively) for  $v_2$  vs.  $KE_T$  for  $\pi^\pm$ ,  $K^\pm$ ,  $(\bar{p})p$ ,  $(\bar{d})d$ , and the  $\phi$  meson, in 20-60% central Au+Au collisions. The left panel clearly shows that, despite its mass which is comparable to that for the proton,  $v_2(KE_T)$  for the  $\phi$  meson follows the flow pattern of the other lighter mesons ( $\pi$  and  $K$ ), whose cross sections are not OZI suppressed. A similar pattern is also observed for the  $v_2(KE_T)$  values inferred for  $D$  mesons (comprised of charmed quarks) from non-photon electron measurements [13, 22]. We interpret these observations as an indication that, when elliptic flow develops, the constituents of the flowing medium are not ordinary hadrons interacting with their standard hadronic cross sections. Instead, they may indicate a state in which partonic collectivity dominates the transverse expansion dynamics of light, strange, and charmed quarks via a common velocity field.

Interestingly, the  $v_2(KE_T)$  results shown for the  $(\bar{d})d$  and the  $\phi$  meson are essentially identical at low  $KE_T$  ( $KE_T \lesssim 1$  GeV), and are in good agreement with those for other charged hadrons, including the pion with a mass  $\sim 13$  times smaller than the deuteron. This strengthens the earlier finding that, for low  $KE_T$ , all particle species exhibit the same  $v_2$  irrespective of their mass [11, 12, 13]. The expected difference between  $(\bar{d})d$  and  $(\bar{p})p$  for  $KE_T \gtrsim 1$  GeV is not tested in Fig. 3, due to the limited  $KE_T$  range of the  $(\bar{d})d$  data.

The right panel of Fig. 3 shows the results for a validation test of universal scaling for  $v_2(KE_T)$  of baryons and mesons [11, 12, 13]. The value  $n_q = 2 \times 3$  is used for  $(\bar{d})d$  to account for its composite ( $p + n$ ) nature. The scaled results shown in Fig. 3b clearly serve as further validation for the experimentally observed universal scaling of  $v_2$  for baryons and mesons [11, 12, 13]. This finding lends strong support to the notion that the high energy density matter, created in RHIC collisions, comprise a pre-hadronization state that contains the prerequisite quantum numbers of the hadrons to be formed. Thus, it appears that partonic collectivity dominates the expansion dynamics of these collisions. The special role of  $KE_T$  as a scaling variable is under investigation.

In summary, we have presented differential  $v_2$  measurements for the  $\phi$  meson and deuteron, and have compared them to those for other mesons and baryons. For a broad range of  $KE_T$  values, the differential  $v_2(KE_T)$  for the  $\phi$  meson follows the flow pattern for other light mesons whose cross sections are not OZI suppressed. The composites  $(\bar{d})d$  follow the flow pattern for baryons with  $v_2$  values which are additive. When  $v_2/n_q$  is plotted as a function of the transverse kinetic energy scaled by the number of valence quarks (ie.  $KE_T/n_q$ ), universal scaling results for all particle species measured. These observations suggest that the transverse expansion dynamics leading to elliptic flow development cannot be understood in terms of ordinary hadrons interacting with their standard hadronic cross sections, but rather in terms of a

pre-hadronization state in which the flowing medium reflects quark degrees of freedom.

We thank the staff of the Collider-Accelerator and Physics Departments at BNL for their vital contributions. We acknowledge support from the Department of Energy and NSF (U.S.A.), MEXT and JSPS (Japan), CNPq and FAPESP (Brazil), NSFC (China), IN2P3/CNRS, and CEA (France), BMBF, DAAD, and AvH (Germany), OTKA (Hungary), DAE (India), ISF (Israel), KRF and KOSEF (Korea), MES, RAS, and FAAE (Russia), VR and KAW (Sweden), U.S. CRDF for the FSU, US-Hungarian NSF-OTKA-MTA, and US-Israel BSF.

---

\* PHENIX Spokesperson: jacak@skipper.physics.sunysb.edu

† Deceased

- [1] K. Adcox et al., Nucl. Phys. **A757**, 184 (2005).
- [2] M. Gyulassy and L. McLerran, Nucl. Phys. **A750**, 30 (2005).
- [3] E. V. Shuryak, Nucl. Phys. **A750**, 64 (2005).
- [4] K. H. Ackermann et al., Phys. Rev. Lett. **86**, 402 (2001).
- [5] K. Adcox et al., Phys. Rev. Lett. **89**, 212301 (2002).
- [6] S. S. Adler et al., Phys. Rev. Lett. **91**, 182301 (2003).
- [7] S. S. Adler et al., Phys. Rev. Lett. **94**, 232302 (2005).
- [8] R. A. Lacey, Nucl. Phys. **A774**, 199 (2006).
- [9] M. Demoulin et al., Phys. Lett. **B241**, 476 (1990).
- [10] S. Voloshin and Y. Zhang, Z. Phys. **C70**, 665 (1996).
- [11] M. Issah and A. Taranenko (2006), nucl-ex/0604011.
- [12] A. Adare et al. (2006), nucl-ex/0608033.
- [13] R. A. Lacey and A. Taranenko (2006), nucl-ex/0610029.
- [14] U. W. Heinz and P. F. Kolb, Nucl. Phys. **A702**, 269 (2002).
- [15] M. Asakawa, S. A. Bass, and B. Muller, Phys. Rev. Lett. **96**, 252301 (2006).
- [16] S. A. Voloshin, Nucl. Phys. **A715**, 379 (2003).
- [17] R. J. Fries, B. Muller, C. Nonaka, and S. A. Bass, Phys. Rev. **C68**, 044902 (2003).
- [18] V. Greco, C. M. Ko, and P. Levai, Phys. Rev. **C68**, 034904 (2003).
- [19] N. Xu, Nucl. Phys. **A751**, 109 (2005).
- [20] B. Müller and J. L. Nagle (2006), nucl-th/0602029.
- [21] M. Oldenburg, J. Phys. **G32**, S563 (2006).
- [22] A. Adare et al. (2006), nucl-ex/0611018.
- [23] S. Okubo, Phys. Lett. **5**, 165 (1963).
- [24] A. Shor, Phys. Rev. Lett. **54**, 1122 (1985).
- [25] C. M. Ko and D. Seibert, Phys. Rev. **C49**, 2198 (1994).
- [26] K. Haglin, Nucl. Phys. **A584**, 719 (1995).
- [27] C. Nonaka et al., Phys. Rev. **C69**, 031902 (2004).
- [28] J. H. Chen et al. (2005), nucl-th/0504055.
- [29] C. Adler et al., Phys. Rev. Lett. **87**, 262301 (2001).
- [30] S. S. Adler et al., Phys. Rev. Lett. **94**, 122302 (2005).
- [31] K. Adcox et al., Nucl. Instrum. Meth. **A499**, 469 (2003).
- [32] K. Adcox et al., Phys. Rev. **C69**, 024904 (2004).
- [33] S. S. Adler et al., Phys. Rev. **C69**, 034909 (2004).
- [34] J. Jia (PHENIX), Nucl. Phys. **A783**, 501 (2007).
- [35] A. M. Poskanzer and S. A. Voloshin, Phys. Rev. **C58**, 1671 (1998).
- [36] N. Borghini and J. Y. Ollitrault, Phys. Rev. **C70**, 064905 (2004).
- [37] S. S. Adler et al., Phys. Rev. **C72**, 014903 (2005).
- [38] D. Pal, Nucl. Phys. **A774**, 489 (2006).
- [39] S. S. Adler et al., Phys. Rev. Lett. **96**, 032302 (2006).